Cell Chemical Biology, Volume *25*

Supplemental Information

Lipids Shape the Electron Acceptor-Binding Site of the Peripheral Membrane Protein Dihydroorotate Dehydrogenase

Joana Costeira-Paulo, Joseph Gault, Gergana Popova, Marcus J.G.W. Ladds, Ingeborg M.M. van Leeuwen, Médoune Sarr, Anders Olsson, David P. Lane, Sonia Laín, Erik G. Marklund, and Michael Landreh

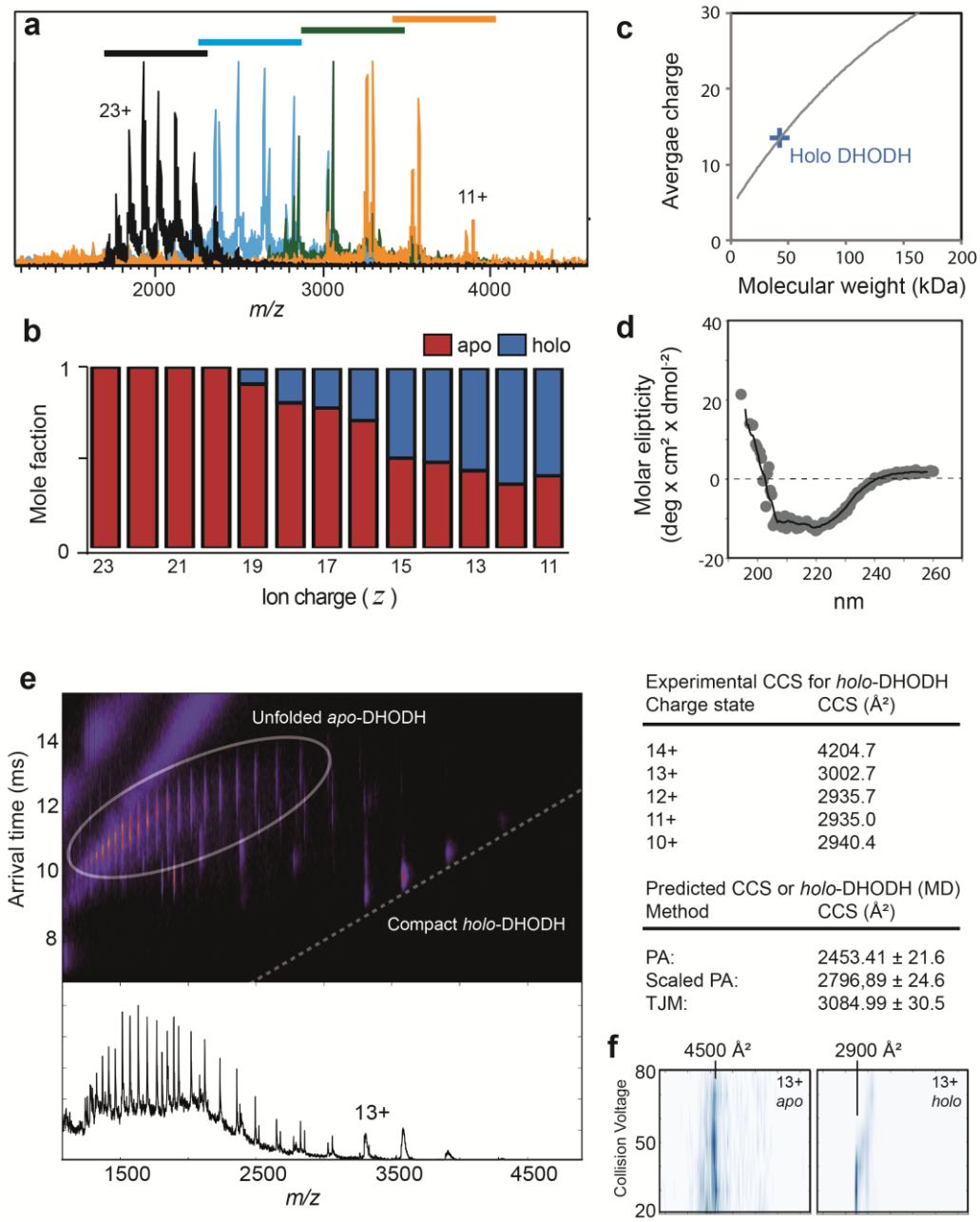

Figure S1. DHODH is folded under MS solution conditions, Related to Figure 1. (a) Sequential isolation of the ions in the range between *m/z* 1400 and 4000 allows analysis of the charge state distributions of apo- and holo-DHODH. Colored bars above the spectra indicate the respective isolation windows. **(b)** Quantification of the molar fractions of apo- and holo-protein for each charge state shown in (a) show a narrow charge state distribution around 14+ for the DHODH-FMN complex. **(c)** Holo DHODH charge states indicate a compact conformation. The expected average charge for an idealized spherical protein with a density of 0.63 g×cm^{-3} is shown as a grey curve (Bush et al., 2010, Kaltashov and

Mohimen, 2005). The average charge state for holo DHODH assuming a mono-modal distribution is indicated in blue. **(d)** The CD spectrum of 10 µM DHODH in MS buffer (100 mM ammonium acetate, pH 7.5, 6 mM LDAO) shows a largely α-helical conformation with no pronounced contributions from random coil content. **(e)** Linear field drift tube ion mobility MS shows that highly charged apo-DHODH is unfolded, while holo-DHODH ionizes with lower average charge and retains a compact conformation. The dotted line indicates the theoretical drift time of a protein with a CCS of 2800 $Å^2$. The CCS values for the N-terminally truncated holo-enzyme are in good agreement with the CCS values predicted based on solution MD of the truncated protein, both by projection approximation (PA) with empirical scaling factor (Bush et al., 2010), as well as by the trajectory method (TJM). **f)** Plotting the non-normalized arrival time distributions for the 13+ charge state of apo- (left) and holo-DHODH (right) against the collision voltage show that gas phase-activation results in loss of FMN rather than unfolding of the holo-enzyme.

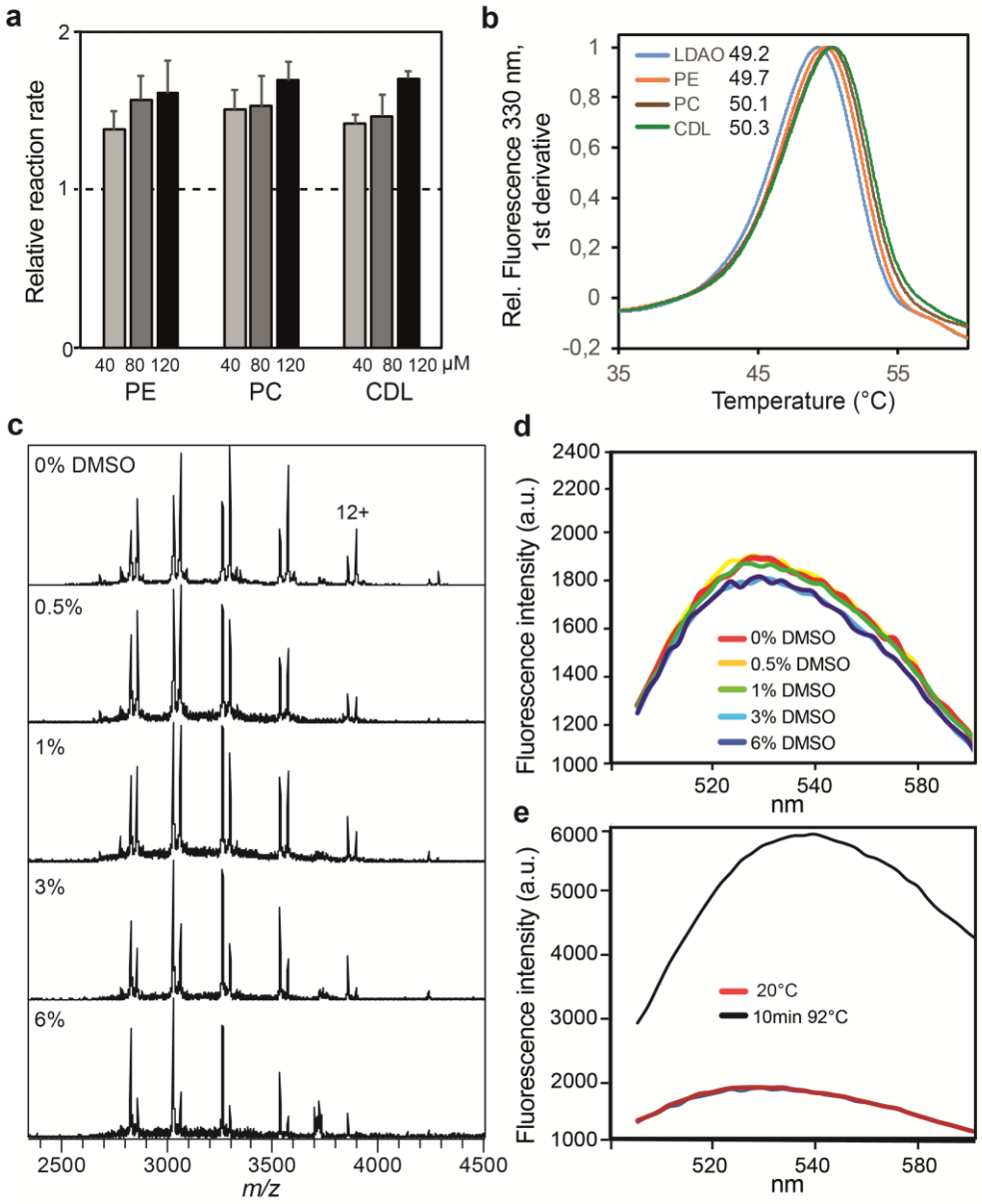

Figure S2. Assessing the stability of lipid and FMN binding in solution and in nESI-MS, Related to Figure 2. (a) Spectrophotometric activity assays measuring the initial reduction rate of benzoquinone show increased activity of the detergent-solubilized protein in the presence of PC, PE, and CDL compared to detergent-only. Error bars indicate average ± standard deviation from three biological repeats and normalized to the V_{max} of DHODH in detergent only. **(b)** Thermal unfolding profiles show no significant effect of PC, PE, or CDL on the thermal stability of DHODH in solution. **(c)** Mass spectra of DHODH show progressive loss of the FMN cofactor at increasing DHODH concentrations, suggesting that even small amounts destabilize interactions with the cofactor under MS conditions. DMSO is enriched in the electrospray droplets, inducing protein unfolding (Cubrilovic and Zenobi, 2013, Sterling et

al., 2011). **(d)** Intrinsic FMN fluorescence in response to increasing DMSO concentrations reveals that the presence of ≥1% DMSO has no pronounced effect the FMN co-factor. **(e)** Thermal denaturation results in significantly increased fluorescence indicating FMN release.

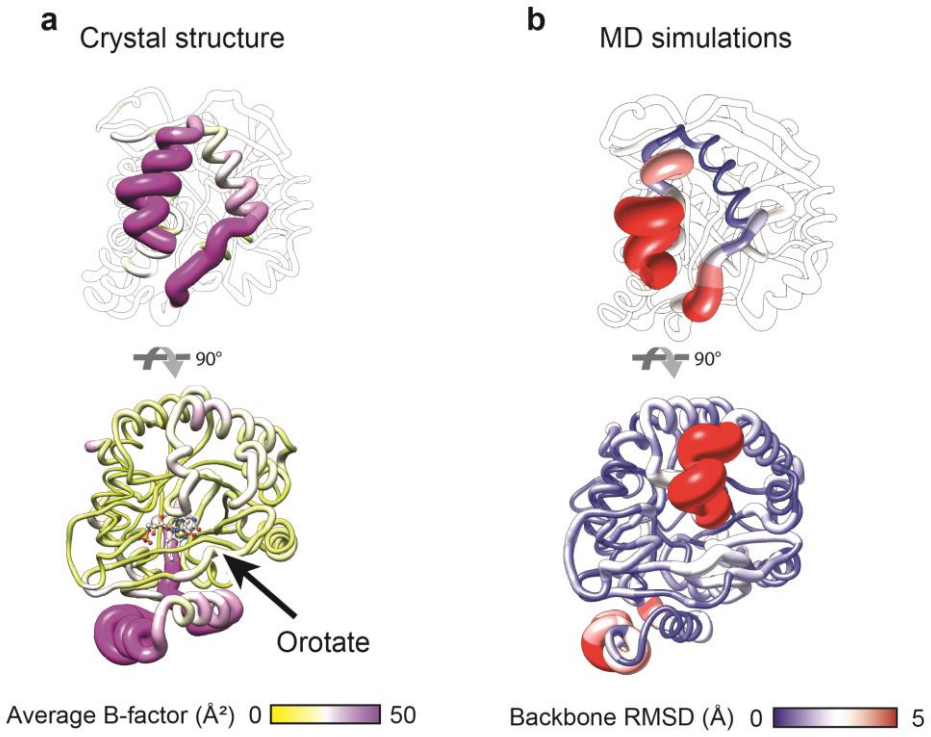

Figure S3. Crystal structures and MD simulations reveal the substrate access sites in DHODH, Related to Figure 3. (a) The crystal structure of DHODH with FMN and orotate (PDB ID 2PRM) exhibits increased local B-factors between residues 214 and 226 hydrogen-bonded to the dihydroorotate substrate. **(b)** The same segment shows large conformational re-arrangements in MD simulations of holo-DHODH without substrate bound.

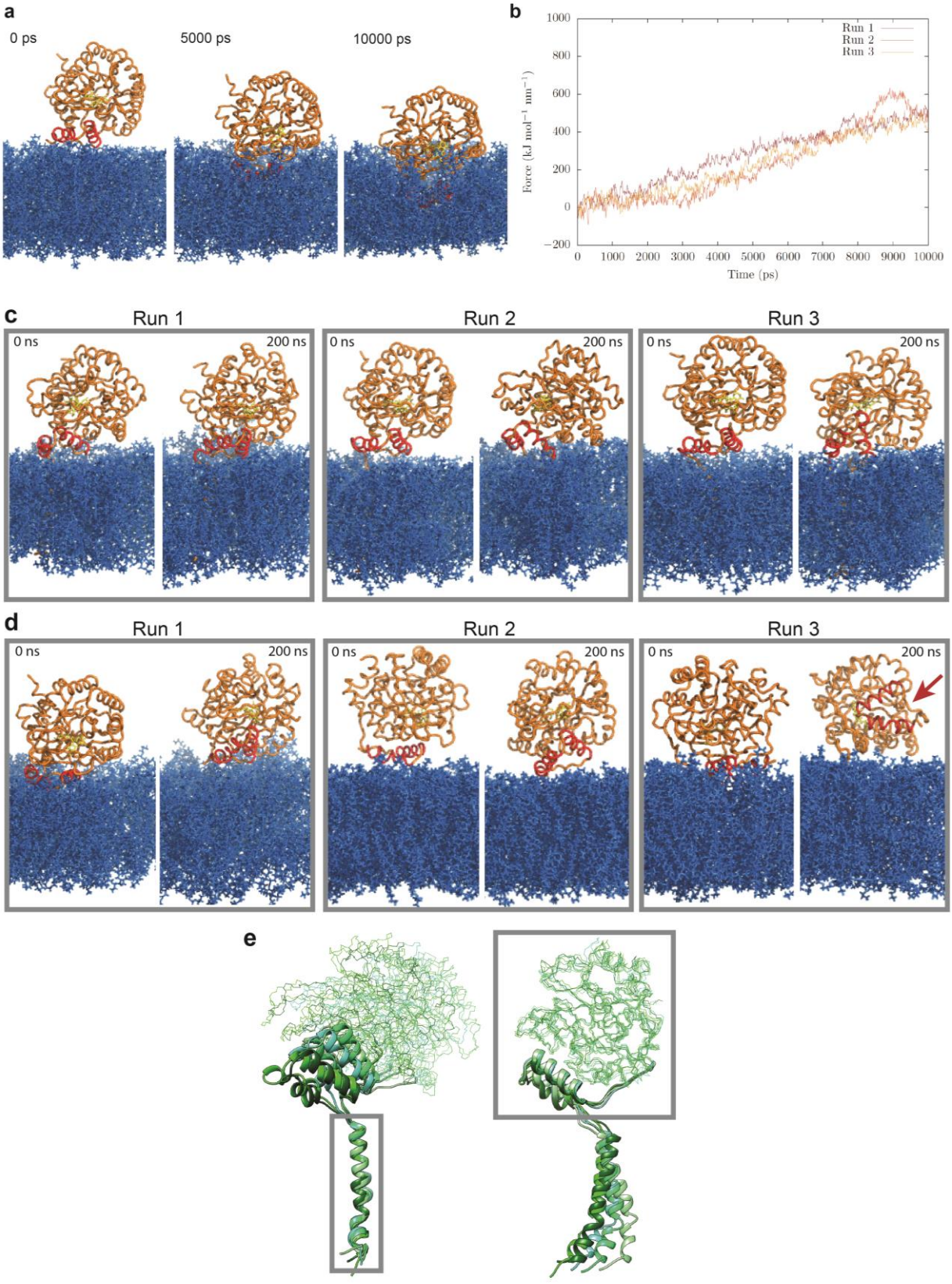

Figure S4. Dynamics of full-length and truncated DHODH on the membrane, Related to Figure 4. (a) The preferred insertion depth of DHDOH in the PE bilayer was determined by pulling the protein towards the center of the bilayer in a 10 ns all-atom simulation. **(b)**

Monitoring the required force reveals a near-linear increase as the protein is inserted into the membrane, indicating that even partial insertion below the lipid head-group region is not energetically favourable. Data is shown for three independent repeats. **(c)** MD simulation start and end structures of full-length DHODH (see methods) converge towards a common orientation on the membrane. **(d)** Using the same experimental setup, truncated DHODH reaches similar orientations in two out of three trajectories, while in the third trajectory, the membrane-binding domain fully detaches from the membrane (arrow). The membrane-binding domain is shown in red. **(e)** The TM helix and the soluble domain of full-length DHDOH can be superimposed independently, indicating a flexible connection. Structures represent snapshots of the protein every 50 ns during the 200 ns trajectory.